School of Pharmaceutical Sciences[1], Sun Yat-sen University, Guangzhou; College of Life Science[2], Shenzhen University, Shenzhen, China

Syntheses of tanshinone anhydrides and their suppression on oxidized LDL uptake in macrophages and foam cell formation

Xiao-Bing Li[1], Xi Cheng[1], Da-Li Zhang[1], Hai-Qiang Wu[2], Jian-Tao Ye[1], Jun Du[1], Zhi-Shu Huang[1], Lian-Quan Gu[1], Lin-Kun An[1]

Received September 10, 2013, accepted October 1, 2013

Dr. Lin-Kun AN, School of Pharmaceutical Sciences, Sun Yat-sen University, Guangzhou, 510006, China
lssalk@mail.sysu.edu.cn

Pharmazie 69: 163–167 (2014) *doi: 10.1691/ph.2014.3839*

We synthesized eight tanshinone anhydrides and the alcoholytic derivatives through a mild oxygen-insertion under Pd/C catalytic hydrogenation conditions. The suppressive effects of the anhydrides on the oxidized low-density lipoprotein (oxLDL) uptake and the oxLDL-induced macrophage-derived foam cell formation were studied. Our results revealed that both anhydrides **1a** and **2a** could significantly suppress the oxLDL uptake in macrophages and the foam cell formation at micromolar level, which might be partially attributed to their inhibition of oxLDL-induced LOX-1 expression in macrophages.

1. Introduction

Atherosclerosis, a leading cause of morbidity and mortality (Lloyd et al. 2010), is a systemic cardiovascular disease characterized by the accumulation of cholesterol and various lipids in the subendothelium, resulting in the narrowing of the vessel lumen (Lusis 2000). In the early stages of atherosclerosis, the uptake and accumulation of lipoproteins, including oxidized low-density lipoprotein (oxLDL), in macrophages result in the formation of foam cell (Brown and Goldstein 1983; Moore and Tabas 2011; Shibata and Glass 2010). Lectin-like oxLDL receptor-1 (LOX-1), a cell surface scavenger receptor highly expressed in human and experimental atherosclerotic lesions, is responsible for the uptake of oxLDL in vascular cells (Aoyama et al. 2000; Sawamura et al. 1997). It has been suggested that down-regulation of LOX-1 expression with the decrease of lipoproteins uptake and accumulation in macrophages may inhibit the macrophage-derived foam cell formation, and plays an important role in the prevention of atherogenesis (Li et al. 2001; Stein et al. 2010).

Tanshinones are the major pharmacological lipophilic active compounds isolated from *Salvia miltiorrhiza* Bunge, a well-known traditional Chinese medicinal herb, and have been widely used for the prevention and management of cardiovascular diseases including atherosclerosis for a long time in Asian countries (Gao et al. 2012). Furthermore, it was reported that tanshinone IIA could suppress oxLDL uptake and prevent atherogenesis in several animal models (Chen et al. 2012; Tang et al. 2011; Xu et al. 2011). Tanshinones might undergo a photooxidative reaction to give their anhydride-type products in plants (Kusumi et al. 1976), which was partially proven by the isolation of several tanshinone anhydrides (Chang et al. 1990; Cao et al. 2009; Lin et al. 1995). Although tanshinone anhydrides were isolated from *Salvia miltiorrhiza* Bunge decades ago, there is not any report on their biological activity, possibly because of their very low content in the herb. Theoretically, tanshinones would be transformed into their anhydride-type products *via* an oxygen-insertion reaction, such as the Baeyer-Villiger oxidation. Since tanshinone anhydrides are oxidation-labile, it is actually difficult to synthesize tanshinone anhydrides in high yield by directly oxidizing tanshinones under a strong oxidative condition. In our previous study, we found that *o*-quinones could be easily transformed into their anhydride-type products in high yield under catalytic hydrogenation conditions (Zhang et al. 2013). Under this mild conditions, tanshinones could be oxygen-inserted and transformed into their anhydride-type derivatives in high yield. And we found that tanshinone anhydrides were stable in ethanol solution or water at room temperature, which stimulated our further investigation on their potential biological activity for the prevention of atherogenesis. In this study, we report the syntheses of tanshinone anhydrides and their suppressive effects on the oxLDL uptake in macrophages and the formation of macrophage-derived foam cells.

2. Investigations and results

2.1. Chemistry

In our previous study, we found a novel oxygen-insertion reaction under catalytic hydrogenation conditions that could easily transform an *o*-quinone into its anhydride product, which might provide a benign method to synthesize anhydride derivatives with a scissile structure under oxidative conditions (Zhang et al. 2013). And if using ethanol as solvent, an anhydride product and an alcoholytic product would be obtained at the same time. To determine the biological activity of tanshinone anhydrides and their corresponding alcoholytic derivatives, they were synthesized according to our reported method as shown in the Scheme. With the assistance of acetic acid, tanshinone IIA (**1**) was transformed into its anhydride (**1a**) and the alcoholytic derivative (**1b**) under Pd/C catalytic hydrogenation condition. The anhydride **1a** was characterized by HRMS, ^{1}H NMR and ^{13}C NMR spectra, which were similar to that of standard sample (Chang et al. 1990; Cao

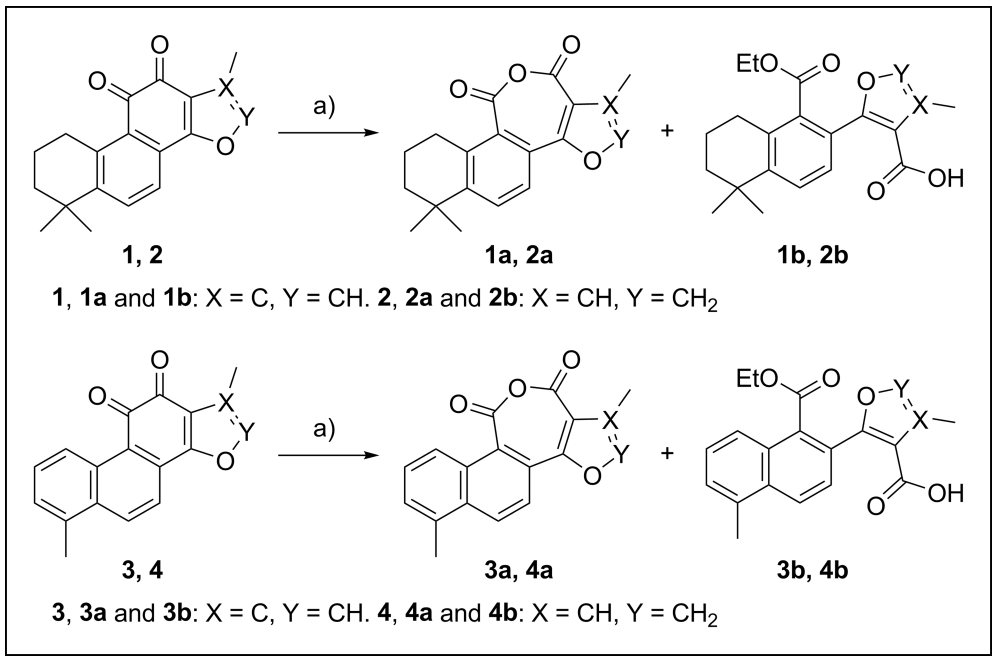

Scheme: Syntheses of tanshinone anhydrides and their alcoholytic derivatives. Condition and reagents: a) Pd/C, EtOH, AcOH, air/H_2 (1:9), 25 °C, 0.5–5 h.

et al. 2009; Lin et al. 1995). Comparison with the spectra of compound **1a**, HRMS and the signals of ^{1}H NMR at 4.12 and 1.12 ppm of compound **1b** implied that there was an extra ethanol moiety within the structure. 2D NMR spectra confirmed compound **1b** as 2-(1-(ethoxycarbonyl)-5,5-dimethyl-5,6,7,8-tetrahydronaphthalen-2-yl)-4-methylfuran-3-carboxylic acid. However, it was found that anhydride **1a** was stable in ethanol solution at room temperature, which implied that the alcoholytic product **1b** might be produced in the radical pathway course of the oxygen-insertion reaction (Zhang et al. 2013).

Under the same reaction conditions, cryptotanshinone (**2**), tanshinone I (**3**) or dihydrotanshinone I (**4**) gave the target products **2a/b**, **3a/b** or **4a/b**, respectively. All compounds were characterized by HRMS, ^{1}H NMR and ^{13}C NMR spectra. Unfortunately, all alcoholytic derivatives **1–4b** were unstable under the storage conditions, and could not be tested for their biological activity.

2.2. Suppression on foam cell formation

The suppressive effect of the anhydrides on the oxLDL-induced macrophage-derived foam cell formation was pre-screened by oil red O straining assay. As shown in Fig. 1, lipid accumulation in RAW264.7 macrophages was observed and the cells displayed typical foamy appearances after incubation with oxLDL for 24 h. The lipid droplet changed small and less after the treatment with 10 μM anhydride **1a** or **2a**, which indicated that the lipid accumulation was partially decreased by the compounds' treatment. And the oxLDL-induced macrophage-derived foam cell formation was attenuated. Anhydrides **3a** and **4a** showed no suppression effect on the lipid accumulation and the foam cell formation (data not shown).

2.3. MTT assay

The cytotoxicity of anhydrides **1a** and **2a** against RAW264.7 macrophages was measured using MTT assay after incubation with the anhydrides (0.4–50 μM) for 48 h. The results indicated that their IC_{50} values were higher than 50 μM. To evaluate their effect on the RAW264.7 macrophage cell viability under the tested condition, MTT assay was conducted in the presence and the absence of the cytotoxic oxLDL. As shown in Fig. 2, at the concentration of 10 μM, anhydrides **1a** and **2a** showed low cytotoxicity with a percentage of cell viability > 90% by pretreatment for 12 h. oxLDL could significantly reduce the viability of RAW264.7 macrophages down to 32%. However, at the concentration of 10 μM, both anhydrides **1a** and **2a** could significantly increase the macrophage cell viability up to 97% and 86%, respectively. This result indicated that both anhydrides **1a** and **2a** showed strong protective effect against oxLDL-induced cytotoxicity in RAW264.7 macrophages.

2.4. Suppression on DiI-oxLDL uptake

To further confirm the effects of anhydrides **1a** and **2a** on the lipid accumulation and the foam cell formation, DiI-oxLDL uptake assays of anhydrides **1a** and **2a** were conducted. The macrophage cells were pretreated with anhydrides followed by incubation with DiI-oxLDL (20 μg/ml) for 6 h. The cellular uptake of DiI-oxLDL was detected under confocal microscopy.

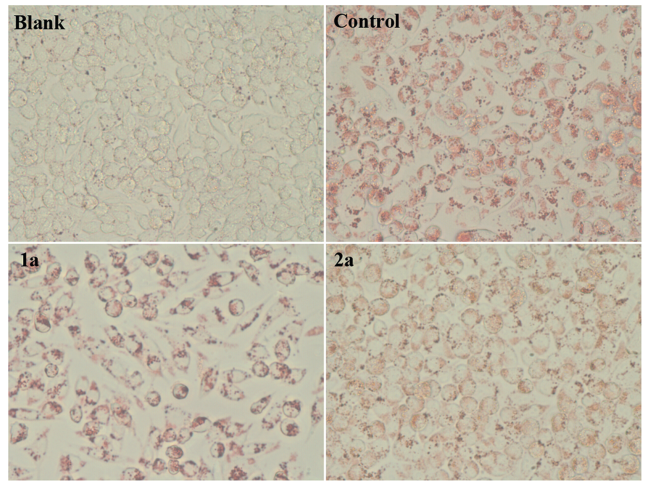

Fig. 1: Effects on oxLDL-induced foam cell formation in RAW264.7 macrophage cell line. The macrophage cells were pre-incubated with anhydrides (10 μM) for 12 h, followed with the treatment of oxLDL (50 μg/ml) for 24 h. The lipid laden macrophage cells (foam cells) were stained for neutral lipids with oil red O. Blank: normal cells (without anhydride and oxLDL treatment). Control: foam cells (only with oxLDL treatment).

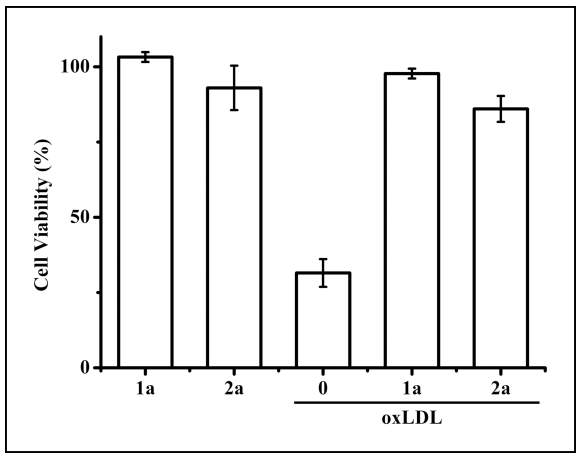

Fig. 2: The effect of tanshinone anhydrides on RAW264.7 macrophage cell viability in the absence or the presence of oxLDL (50 μg/mL). In the absence of oxLDL, cells were serum starved for 12 h and pre-incubated with anhydrides for 12 h. In the presence of oxLDL, cells were serum starved for 12 h and pre-incubated with anhydrides for 12 h, and then treated with oxLDL for 24 h. The cell viability was measured by MTT assay.

As shown in Fig. 3, the uptake of DiI-oxLDL into RAW264.7 macrophages was obviously observed after incubation with DiI-oxLDL. After pretreatment with both anhydrides **1a** and **2a**, the uptake of DiI-oxLDL in RAW264.7 macrophages were obviously inhibited in dose-dependent manner, which implied that the suppression of anhydrides on the lipid accumulation and the foam cell formation might be attributed to the inhibition on oxLDL uptake.

2.5. Effect on LOX-1 expression

LOX-1 is one of the crucial types of scavenger receptor involved in the uptake of modified LDL, including oxLDL, into macrophages. Furthermore, over-expression of LOX-1 has been demonstrated to be closely associated with the macrophage-derived foam cell formation and subsequent development of atherosclerosis. Fig. 4 shows that both anhydrides **1a** and **2a** could obviously reduce oxLDL-induced LOX-1 protein expression in dose-dependent. The Western Blot result indicated that the suppressive effects of both anhydrides **1a** and **2a** on the oxLDL uptake and the foam cell formation might be partially attributed to their inhibition of oxLDL-induced LOX-1 expression in macrophages, which is similar to that of tanshinone IIA (Xu et al. 2012).

2.6. Conclusion

In summary, we synthesized eight tanshinone anhydrides and the alcoholytic derivatives, and firstly studied the suppression of anhydrides on the oxLDL uptake and the foam cell formation. Our studies revealed that both anhydrides **1a** and **2a** could significantly suppress the oxLDL uptake and the oxLDL-induced macrophage-derived foam cell formation at micromolar level, which might be partially attributed to the inhibition of LOX-1 expression in macrophages. This result indicates the potential protection of tanshinone anhydrides **1a** and **2a** against atherosclerosis.

3. Experimental

3.1. General experiments

All solvents were obtained from commercial suppliers and used without further purification unless mentioned. Pd/C (10%) was purchased from Acros Organics. Tanshinone IIA (**1**), cryptotanshinone (**2**), tanshinone I (**3**) and

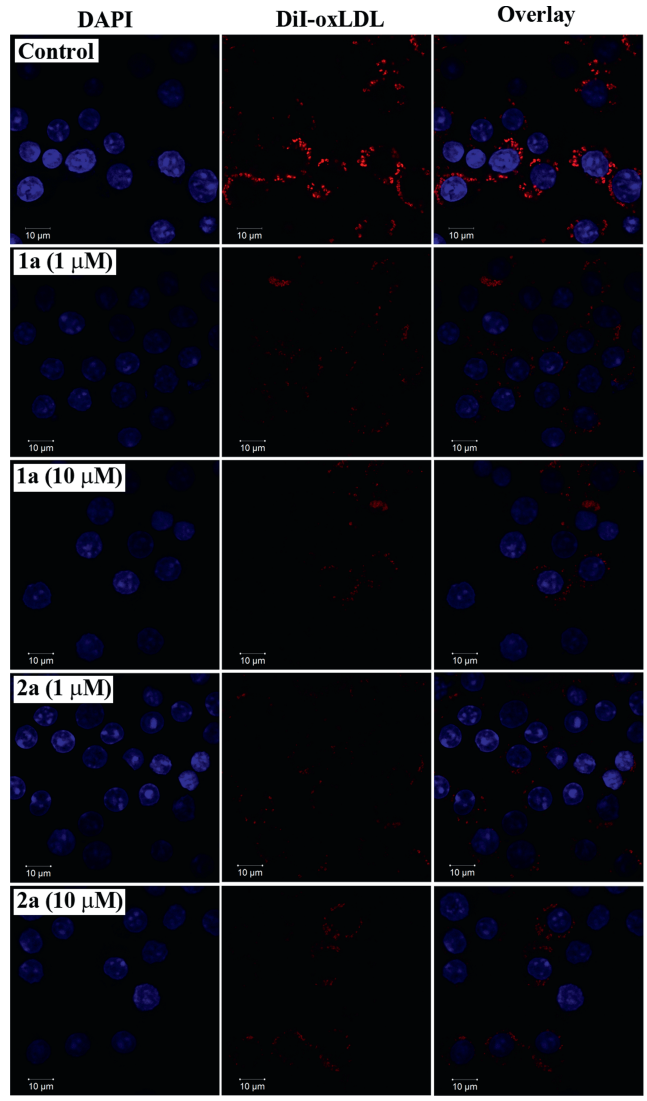

Fig. 3: The effect on DiI-oxLDL uptake in RAW264.7 macrophages. The cells were serum starved for 12 h and pre-incubated with anhydrides for 12 h, and then treated with DiI-oxLDL (20 μg/ml) for 6 h. Subsequently, cells were fixed and analyzed by confocal microscopy. Control: cells pre-incubated with DiI-oxLDL without anhydride.

dihydrotanshinone I (**4**) were isolated from the Chinese medicinal herb, *S. miltiorrhiza* Bunge by our lab (An et al. 2002). Silica gel column chromatography was carried out with silica gel (200–300 mesh). Nuclear magnetic resonance spectra were recorded on Bruker AVANCE III 400 MHz spectrometer using tetramethylsilane as the internal standard. Mass spectra were analyzed on an Agilent LC-MS 6120 (Quadrupole LC-MS) mass spectrometer. High-resolution mass spectra (HRMS) were analyzed on a SHIMADZU LCMS-IT-TOF mass spectrometer. The purities of the tested compounds were more than 95%, analyzed by High Performance Liquid Chromatography (HPLC) on SHIMADZU LC-20A equipped with a reverse-phase Waters Sunfire C_{18} column, 5 μm, 4.6 x 250 mm.

3.2. Syntheses of compounds 1-4a/b

To a 50 ml round-bottomed flask, a suspension of tanshinone (0.10 mmol) and 10% Pd/C (3 mg) in EtOH (20 ml) was added. The mixture was added with acetic acid (0.3 ml) by syringe. The flask was charged with the mixture gas of air and hydrogen (1:9). The reaction solution was stirred at 25 ^{O}C for 0.5–5 h. The reaction course was monitored by HPLC. After the reaction was stopped, the reaction solution was filtered and concentrated under reduced pressure. The residue was purified by silicon gel column chromatography using ethyl acetate/petroleum ether (1:20∼1:5) mixture as eluent to give the target anhydride and alcoholytic derivatives.

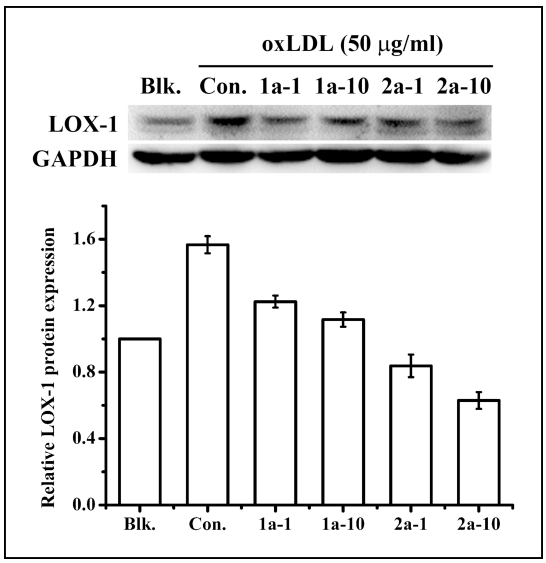

Fig. 4: Inhibitory effects of anhydrides (1 μM and 10 μM) on oxLDL induced LOX-1 protein expression. RAW264.7 cells were serum starved for 12 h and pretreated with anhydrides 1a (1 μM and 10 μM) and 2a (1 μM and 10 μM) separately for 6 h followed by exposure to oxLDL (50 μg/ml) for a further 24 h period. At the end of the incubation period. LOX-1 protein expression by western blotting were evaluated. Blk.: normal cells (without anhydride and oxLDL treatment). Con.: cells treated with oxLDL.

3.2.1. 4,9,9-Trimethyl-9,10,11,12-tetrahydrofuro[3,2-c]naphtho[2,1-e]oxepine-1,3-dione (1a)

White solid (149 mg, 48%). Mp = 150.6–152.4 °C (from petroleum ether 15:1 /ethyl acetate, lit: 148–150 °C [17], 137–140 °C [14]). ^{1}H NMR (400 MHz, $CDCl_3$) δ 7.65 (d, AB, J = 8.4 Hz, 1H), 7.62 (d, AB, J = 8.4 Hz, 1H), 7.33 (q, J = 1.2 Hz, 1H), 2.88 (t, J = 6.4 Hz, 2H), 2.27 (d, J = 1.2 Hz, 3H), 1.88–1.81 (m, 2H), 1.72–1.69 (m, 2H), 1.33 (s, 6H) [15,18]. ^{13}C NMR (100 MHz, $CDCl_3$) δ 162.6, 155.6, 155.0, 149.7, 140.6, 135.7, 130.6, 128.6, 123.4, 122.8, 122.4, 113.5, 38.2, 34.7, 31.7, 28.3, 19.0, 8.9. HRMS (ESI) *m/z*: calcd for $C_{19}H_{19}O_4$ 311.1283 $[M+H]^+$; found: 311.1283.

3.2.2. 2-(1-(Ethoxycarbonyl)-5,5-dimethyl-5,6,7,8-tetrahydronaphthalen-2-yl)-4-methylfuran-3-carboxylic acid (1b)

Yellow oil (139 mg, 39%), ^{1}H NMR (400 MHz, Acetone-d_6) δ 7.53 (d, J = 8.4 Hz, 1H), 7.39 (s, 1H), 7.38 (d, J = 8.0 Hz, 1H), 4.12 (q, J = 7.2 Hz, 2H), 2.84 (t, J = 6.2 Hz, 2H), 2.17 (s, 3H), 1.86–1.80 (m, 2H), 1.72–1.69 (m, 2H), 1.333 (s, 3H), 1.328 (s, 3H), 1.12 (t, J = 7.0 Hz, 3H). ^{13}C NMR (100 MHz, Acetone-d_6) δ 170.0, 164.2, 158.4, 148.4, 140.5, 135.4, 133.8, 129.1, 127.9, 126.9, 122.7, 116.0, 60.5, 39.3, 35.0, 32.1, 28.9, 20.0, 14.1, 10.0. HRMS (ESI) *m/z*: calcd for $C_{21}H_{24}O_5Na$ 379.1516 $[M+Na]^+$; found 379.1510.

3.2.3. 4,9,9-Trimethyl-4,5,9,10,11,12-hexahydrofuro[3,2-c]naphtho[2,1-e]oxepine-1,3-dione (2a)

White solid (140 mg, 45%). Mp = 181.0–182.0 °C (from petroleum ether 15:1 ethyl acetate, lit: 153–155 °C [17], 183–184 °C [18]). $[\alpha]_D^{20} = 101.0$ (c = 1.0 mg/ml, CH_2Cl_2). ^{1}H NMR (400 MHz, $CDCl_3$) δ 7.59 (s, 2H), 4.75 (dd, J = 9.6, 9.2, 1H), 4.20 (dd, J = 9.0, 7.0 Hz, 1H), 3.64–3.57 (m, 1H), 2.98–2.92 (m, 1H), 2.80–2.74 (m, 1H), 1.89–1.79 (m, 2H), 1.70–1.68 (m, 2H), 1.35 (d, J = 6.8 Hz, 3H), 1.33 (s, 3H), 1.31 (s, 3H) [15,18]. ^{13}C NMR (100 MHz, $CDCl_3$) δ 163.8, 163.0, 156.5, 151.7, 135.4, 130.3, 130.1, 123.5, 122.2, 108.7, 78.0, 38.4, 38.1, 34.8, 31.7, 31.6, 28.3, 19.0, 18.7. HRMS (ESI) *m/z*: calcd for $C_{19}H_{21}O_4$ 313.1440 $[M+H]^+$; found: 313.1440.

3.2.4. 2-(1-(Ethoxycarbonyl)-5,5-dimethyl-5,6,7,8-tetrahydronaphthalen-2-yl)-4-methyl-4,5-dihydrofuran-3-carboxylic acid (2b)

White gel (150 mg, 42%). $[\alpha]_D^{20} = 71.7$ (c = 1.0 mg/ml, CH_2Cl_2). ^{1}H NMR (400 MHz, Acetone-d_6) δ 7.48 (d, J = 8.0 Hz, 1H), 7.32 (d, J = 8.4 Hz, 1H), 4.50 (t, J = 9.2 Hz, 1H), 4.09 (dd, J = 9.0, 4.6 Hz, 1H), 3.97 (q, J = 7.2 Hz, 2H), 3.36–3.27 (m, 1H), 2.93–2.83 (m, 1H), 2.81–2.73 (m,1H), 1.82–1.78 (m, 2H), 1.72–1.67 (m, 2H), 1.31 (s, 6H), 1.24 (d, J = 6.4 Hz, 3H), 1.04 (t, J = 7.2 Hz, 3H). ^{13}C NMR (100 MHz, Acetone-d_6) δ 169.7, 166.2, 165.2, 148.8, 134.8, 133.8, 128.6, 127.8, 127.6, 110.7, 78.7, 59.7, 39.4, 38.9, 35.0, 32.13, 32.11, 28.9, 20.0, 19.8, 14.2. HRMS (ESI) *m/z*: calcd for $C_{21}H_{25}O_5$ 357.1702 $[M-H]^-$; found: 357.1693.

3.2.5. 4,9-Dimethylfuro[3,2-c]naphtho[2,1-e]oxepine-1,3-dione (3a)

White solid (123 mg, 42%). Mp = 161.2–162.1 °C, (from CH_2Cl_2, lit [17]: 171–173 °C). ^{1}H NMR (400 MHz, $CDCl_3$) δ 8.26 (d, J = 8.8 Hz, 1H), 7.98 (d, J = 8.4 Hz, 1H), 7.94 (d, J = 9.2 Hz, 1H), 7.56–7.52 (m, 1H), 7.46–7.44 (m, 1H), 7.42 (s, 1H), 2.73 (s, 3H), 2.32 (s, 3H). ^{13}C NMR (100 MHz, $CDCl_3$) δ 162.0, 155.3, 154.7, 141.2, 135.0, 133.0, 130.0, 129.0, 128.7, 126.6, 123.9, 123.7, 123.3, 120.5, 114.6, 19.5, 8.9. HRMS (ESI) *m/z*: calcd for $C_{18}H_{12}O_4Na$ 315.0628 $[M+Na]^+$; found: 315.0622.

3.2.6. 2-(1-(Ethoxycarbonyl)-5-methylnaphthalen-2-yl)-4-methylfuran-3-carboxylic acid (3b)

Yellow oil (105 mg, 31%), ^{1}H NMR (400 MHz, Acetone-d_6) δ 8.12 (d, J = 8.4 Hz, 1H), 7.72 (d, J = 8.8 Hz, 1H), 7.69 (d, J = 8.8 Hz, 1H), 7.49 (s, 1H), 7.41–7.33 (m, 2H), 4.38–4.27 (m, 2H), 3.03 (s, 3H), 2.65 (s, 3H), 1.26 (t, J = 7.2 Hz, 3H). ^{13}C NMR (100 MHz, Acetone-d_6) δ 169.0, 148.5, 147.0, 141.1, 135.2, 133.9, 128.1, 126.6, 125.4, 121.1, 120.0, 118.6, 117.9, 115.2, 109.4, 99.4, 63.1, 19.7, 14.4, 8.3. HRMS (ESI) *m/z*: calcd for $C_{20}H_{19}O_5$ 339.1227 $[M+H]^+$; found 339.1239.

3.2.7. 4,9-Dimethyl-4,5-dihydrofuro[3,2-c]naphtho[2,1-e]oxepine-1,3-dione (4a)

White solid (141 mg, 48%). Mp = 132.6–133.8 °C (from CH_2Cl_2). $[\alpha]_D^{20} = 77.4$ (c = 1.0 mg/ml, CH_2Cl_2). ^{1}H NMR (400 MHz, $CDCl_3$) δ 8.24 (d, J = 8.8 Hz, 1H), 8.01 (d, J = 8.8 Hz, 1H), 7.86 (d, J = 9.2 Hz, 1H), 7.57–7.53 (m, 1H), 7.50–7.48 (m, 1H), 4.83 (t, J = 9.6 Hz, 1H), 4.28 (dd, J = 8.2, 7.4 Hz, 1H), 3.74–3.65 (m, 1H), 2.73 (s, 3H), 1.41 (d, J = 6.8 Hz, 3H) [15]. ^{13}C NMR (100 MHz, $CDCl_3$) δ 163.7, 162.4, 156.2, 134.9, 134.0, 129.5, 129.4, 129.2, 128.6, 128.4, 124.0, 122.8, 121.2, 109.9, 78.2, 38.6, 19.5, 18.6. HRMS (ESI) *m/z*: calcd for $C_{18}H_{14}O_4Na$ 317.0784 $[M+Na]^+$; found: 317.0787.

3.2.8. 2-(1-(Ethoxycarbonyl)-5-methylnaphthalen-2-yl)-4-methyl-4,5-dihydrofuran-3-carboxylic acid (4b)

Yellow oil (119 mg, 35%), ^{1}H NMR (400 MHz, Acetone-d_6) δ 8.16 (d, J = 8.8 Hz, 1H), 8.08 (d, J = 8.4 Hz, 1H), 7.66 (d, J = 8.4 Hz, 1H), 7.48 (t, J = 12.8 Hz, 1H), 7.48 (d, J = 12.0 Hz, 1H), 4.61 (t, J = 9.2 Hz, 1H), 4.20 (dd, J = 6.8, 4.6 Hz, 1H), 4.01–3.93 (m, 2H), 3.43–3.37 (m, 1H), 2.73 (s, 3H), 1.31 (d, J = 6.8 Hz, 3 Hz), 0.97 (t, J = 7.2 Hz, 3H). ^{13}C NMR (100 MHz, Acetone-d_6) δ 169.2, 165.9, 165.2, 135.4, 133.8, 133.3, 130.5, 128.7, 128.5, 127.7, 125.8, 125.1, 111.4, 79.1, 59.9, 39.0, 19.7, 19.6, 14.3. HRMS (ESI) *m/z*: calcd for $C_{20}H_{20}O_5Na$ 363.1203 $[M+Na]^+$; found 363.1186.

3.3. Cell culture and MTT assay

RAW 264.7 cells were cultured in 96-well plates (Costar, Corning, NY) at a density of 5 x 10^4 cells/mL in RPMI 1640 medium (with 100 IU/mL of penicillin G, 100 μg/mL streptomycin, 2 mM L-glutamine, and 10% (v/v) heat-inactivated fetal bovine serum), incubated in a humidified atmosphere of 5% CO_2 in incubator at 37 °C. To evaluate the cytotoxicity of the tanshinone anhydrides, cells were exposed to the anhydrides for 48 h and measured using the MTT assay.

To determine the effect of anhydrides on oxLDL-induced cytotoxicity, cells were starved in RPMI 1640 medium without FBS for 12 h, and were pre-incubated with anhydrides (10 μM) for 12 h before being treated with oxLDL (50 μg/mL) for 24 h to induce cytotoxicity. The cell viability was measured using MTT assay.

3.4. LDL isolation and modification

The use of human plasma (from Guangzhou General Hospital of Guangzhou Military Command) conforms to the principles outlined in the Declaration of Helsinki. Human native-LDL (d = 1.019 to 1.063 g/mL) was prepared from the plasma of normolipidemic volunteers by sequential ultracentrifugation (Xu et al. 2009). LDL was extensively dialyzed for 24 h at 4 °C in Tris buffer (20 mM Tris, 150 mM NaCl, 300 μM EDTA). LDL was oxidized with 10 μM $CuSO_4$ for 24 h to generate oxLDL followed by dialysis against PBS (5 mM Tris, 50 nM NaCl) with 10 μM EDTA and then PBS to remove EDTA. The quality of LDL and oxLDL were monitored by agarose gel electrophoresis. The relative electrophoretic mobility of oxLDL was 2.5 to 2.7 relative to native LDL. The protein content of all lipoproteins was determined using BCA Protein Assay Kit (Thermo) using BSA as a standard. All lipoproteins were filter sterilized, stored at 4 °C in dark and used within 3 weeks.

3.5. Treatment of compounds and oil red O staining

The subconfluent RAW264.7 cells were serum starved for 12 h, and then pretreated with compounds for 12 h in RPMI 1640 medium without FBS

before treatment with oxLDL (50 μg/mL) for 24 h. Foam cell formation was revealed by oil red O staining according to the reported method (Xu et al. 2010). Briefly, cells were fixed in phosphate buffered 10% formalin for 10 min and washed once with PBS. After flushing with 60% isopropanol for 30 s at room temperature, the cells were stained with 0.5% oil red O (Sigma) in 60% isopropanol for 20 min (37 °C, in darkness) and washed once with 60% isopropanol for 5 s. Photomicrographs were taken by phase contrast microscopy with a x40 objective (CKX41; Olympus, Tokyo, Japan). The accumulated lipid in cytoplasm was red with oil red O stained.

3.6. Preparation and uptake of DiI-oxLDL

LDL was labeled with fluorescent probe, 1,1'-dioctadecyl-3,3,3',3'-tetramethyl-indocarbocyanine perchlorate (DiI) according to the reported method with minor modifications (Lian et al. 2008). Briefly, LDL was incubated overnight at 37 °C under nitrogen and light protection with 50 μL of DiI (3 mg/ml in DMSO) for each milligram of LDL protein. Unbound dye was removed by ultracentrifugation at 46,000 rpm for 5.5 h at 4 °C. For preparation of DiI-oxLDL, DiI-LDL (0.9 mg/ml) was incubated with 10 μM $CuSO_4$ (final concentration) at 37 °C in the dark for 24 h. The DiI-oxLDL distributed in the middle layer was re-isolated and subjected to dialysis against phosphate buffered saline containing 0.24 mM EDTA. The protein content of DiI-oxLDL was determined using BCA Protein Assay Kit (Thermo).

To assess the cellular DiI-oxLDL uptake, RAW264.7 macrophage cells were seeded overnight on confocal dishes (Corning, NY) at a density of 5 x 10^5 cells/mL, then were serum starved for 12 h and pre-incubated with the tested compounds or control (0.1% DMSO) for 12 h, and then loaded with DiI-oxLDL (20 μg/mL) for another 6 h at 37 °C. At the end of incubation period, cells were washed once with PBS (with 2 mg/ml BSA) and twice with PBS, then were fixed in phosphate buffered 10% formalin for 10 min. Thereafter, for nucleus staining, the cells were incubated for 20 min with 10 μg/ml DAPI (Sigma) and washed 3 times with PBS. The cells were then placed for confocal microscopy with a x100 oil immersion objective using a 546 nm filter set (LSM 710, ZEISS, Germany), and quantitatively analyzed by flow cytometry.

3.7. Western blot analysis

RAW 264.7 cells were cultured in 96-well plates (Costar, Corning, NY) at a density of 6 x 10^5 cells/mL in RPMI 1640 medium (with 100 IU/mL of penicillin G, 100 μg/mL streptomycin, 2 mM L-glutamine, and 10% (v/v) heat-inactivated fetal bovine serum), incubated in a humidified atmosphere of 5% CO_2 in incubator at 37 °C. RAW264.7 macrophage cells were pretreated with anhydrides for 6 h before stimulation with oxLDL (50 μg/mL) for 24 h. Cells were lysed in lysis buffer containing PMSF (Sigma), and 40 μg proteins were loaded and separated on a 10% SDS-PAGE, then transferred to PVDF membrane as described (Xu et al. 2009). The membrane was probed with a rabbit anti-mouse LOX-1 antibody (1:1000), followed by incubation with an HRP-conjugated anti-rabbit secondary antibody (1:3000, Cell Signaling). Immunocomplexes were detected by ECL method (Pierce). GAPDH was used to normalize the protein loading.

Acknowledgements: This work was financially supported by Natural Science Foundation of China (No. 81373257), Guangdong Provincial Science and Technology Projects (No. 2012B031800114) and the Fundamental Research Funds for the Central Universities.

References

Aoyama T, Chen M, Fujiwara H, Masaki T, Sawamura T (2000) LOX-1 mediates lysophosphatidylcholine-induced oxidized LDL uptake in smooth muscle cells. FEBS Lett 467: 217–220.

An LK, Bu XZ, Wu HQ, Guo XD, Ma L, Gu LQ (2002) Reaction of tanshinones with biogenic amine metabolites *in vitro*. Tetrahedron 58: 10315–10321.

Brown MS, Goldstein JL (1983) Lipoprotein metabolism in the macrophage: Implications for cholesterol deposition in atherosclerosis. Annu Rev Biochem 52: 223–261.

Chang HM, Cheng KP, Choang TF, Chow HF, Chui KY, Hon PM, Tan FWL, Yang Y, Zhong ZP (1990) Structure Elucidation and Total Synthesis of New Tanshinones Isolated from Salvia miltiorrhiza Bunge (Damhen). J Org Chem 55: 3537–3543.

Cao CQ, Sun LR, Wang XN (2009) Chemical constituents of Salvia miltiorrhiza f. alba. Chin Tradit Herbal Drugs 40: 173–175.

Chen WY, Tang FT, Xie BL, Chen SR, Huang HQ, Liu PQ (2012) Amelioration of atherosclerosis by tanshinone IIA in hyperlipidemic rabbits through attenuation of oxidative stress. Eur J Pharmacol 674: 359–364.

Gao S, Liu ZP, Li H, Little PJ, Liu PQ, Xu SW (2012) Cardiovascular actions and therapeutic potential of tanshinone IIA. Atherosclerosis 220: 3–10.

Kusumi T, Kishi T, Kakisawa H (1976) Photo-oxidation of tanshinone II (6,7,8,9-tetrahydro-1,6,6-trimethylphenanthro[1,2-*b*]furan-10,11-dione). J Chem Soc, Perkin Trans 1 1716–1718.

Lin HC, Chang WL, Chen CF (1995) Phytochemical and pharmacological study on Salvia miltiorrhiza (VI)-cytotoxic activity of tanshinones. Chin Pharm J 47: 77–80.

Lusis AJ (2000) Atherosclerosis. Nature 407: 233–241.

Li DY, Chen HJ, Mehta JL (2001) Statins inhibit oxidized-LDL mediated LOX-1 expression, uptake of oxidized-LDL and reduction in PKB phosphorylation. Cardiovasc Res 52: 130–135.

Lian TW, Wang L, Lo YH, Huang IJ, Wu MJ (2008) Fisetin, morin and myricetin attenuate CD36 expression and oxLDL uptake in U937-derived macrophages. Biochim Biophys Acta 1781: 601–609.

Lloyd-Jones D, Adams RJ, Brown TM, Carnethon M, Dai S, De Simone G, Ferguson TB, Ford E, Furie K, Gillespie C, et al (2010) Executive Summary: Heart Disease and Stroke Statistics—2010 Update. Circulation 121: 948–954.

Moore KJ, Tabas I (2011) Macrophages in the pathogenesis of atherosclerosis. Cell 145: 341–355.

Sawamura T, Kume N, Aoyama T, Moriwaki H, Hoshikawa H, Aiba Y, Tanaka T, Miwa S, Katsura Y, Kita T, Masaki T (1997) An endothelial receptor for oxidized low-density lipoprotein. Nature 386: 73–77.

Shibata N, Glass CK (2010) Macrophages, oxysterols and atherosclerosis. Circ J 74: 2045–2051.

Stein S, Lohmann C, Schafer N, Hofmann J, Rohrer L, Besler C, Rothgiesser KM, Becher B, Hottiger MO, Boren J, McBurney MW, Landmesser U, Luscher TF, Matter CM (2010) SIRT1 decreases Lox-1-mediated foam cell formation in atherogenesis. Eur Heart J 31: 2301–2309.

Tang FT, Cao Y, Wang TQ, Wang LJ, Guo J, Zhou XS, Xu SW, Liu WH, Liu PQ, Huang HQ (2011) Tanshinone IIA attenuates atherosclerosis in $ApoE^{-/-}$ mice through down-regulation of scavenger receptor expression. Eur J Pharmacol 650: 275–284.

Xu SW, Fu JJ, Chen JW, Xiao PX, Lan T, Le K, Cheng F, He L, Shen XY, Huang HQ, Liu PQ (2009) Development of an optimized protocol for primary culture of smooth muscle cells from rat thoracic aortas. Cytotechnology 61: 65–72.

Xu SW, Huang Y, XieY, Lan T, Le K, Chen JW, Chen SR, Gao S, Xu XZ, Shen XY, Huang HQ, Liu PQ (2010) Evaluation of foam cell formation in cultured macrophages: an improved method with Oil Red O staining and DiI-oxLDL uptake. Cytotechnology 62: 473–481.

Xu SW. Little PJ, Lan T, Huang Y, Le K, Wu XQ, Shen XY, Huang HQ, Cai Y, Tang FT, Wang H, Liu PQ (2011) Tanshinone II-A attenuates and stabilizes atherosclerotic plaques in apolipoprotein-E knockout mice fed a high cholesterol diet. Arch Biochem Biophys 515: 72–79.

Xu SW, Liu ZP, Huang Y, Le K, Tang FT, Huang HQ, Ogura S, Little PJ, Shen XY, Liu PQ (2012) Tanshinone II-A inhibits oxidized LDL-induced LOX-1 expression in macrophages by reducing intracellular superoxide radical generation and NF-kB activation. Transl Res 160: 114–124.

Zhang DL, Zhou LY, Quan JM, Zhang W, Gu LQ, Huang ZS, An LK (2013) Oxygen-insertion of *o*-quinone under catalytic hydrogenation conditions. Org Lett 15: 1162–1165.